6.1 ESTMIATE OF RADIATIVE FORCING OF BIOMASS BURNING AEROSOLS IN SOUTH ASIAN REGION DURNING THE PERIOD OF TRACE-P

Sheng-Hsiang Wang and Neng-Huei Lin *
Department of Atmospheric Sciences, National Central University, Chung-Li, Taiwan

1. INTRODUCTION

Atmospheric aerosols play an important role in atmospheric energy balance and climate change. Aerosols affect climate through their direct interaction with solar and terrestrial radiation (direct aerosol effect) and through their effect on the optical properties and life cycle of clouds (indirect aerosol effect)(Chylek and Wong,1995). The radiative forcing due to the direct effect of aerosols from biomass burning remains a large uncertainty (IPCC, 2001). However, based on earlier studies Haywood et al. (2000) estimated the radiative forcing due to biomass burning to be in the range of -0.14 ~ -0.74 W m^{-2}. Most of previous studies applied global models to estimate the direct radiative impact of biomass burning aerosols. In this study, we use a regional transport model coupled with a high-resolution solar radiative transfer model to estimate monthly mean radiative impact of biomass burning aerosols on south Asian region. The variation of aerosol spectral optical properties and organic carbon (OC) aerosol size change with local relative humidity was considered in this study. We also compare our results with respect to various biomass burning sources, i.e. black carbon (BC), and organic carbon emission.

Corresponding author address: Prof. Neng-Huei Lin, National Central Univ., Dept. of Atmospheric Sciences, Chung-Li, Taiwan; e-mail: nhlin@cc.ncu.edu.tw

2. METHODOLOGY AND DATA USED

We combined the USA NOAA HYbrid Single-Particle Lagrangian Integrated Transport model (HYSPLIT) and a high-resolution solar radiative transfer model (CLIRAD-SW, Chou et al. (1999)) to estimate the radiative impact due to the aerosols from the Asian biomass burning. The model domain is between 70°-140°E, 0–50°N, covering South and East Asian. The meteorological data adopted is NCEP's AVN with a spatial resolution of 191km and a time resolution of 6 hrs. The simulation period is March 1–28, 2001.

2.1 HYSPLIT Model

HYSPLIT model was used for calculating the trajectories of air parcels and the transport, dispersion and deposition of pollutant particles/puff (Draxler et al., 2001). In this study, the dispersion of pollutant was configured as Top-Hat Puff simulation. Daily emissions of BC and OC from biomass burning sources were based on the work of Streets et al. (2003), which was estimated for Asian region during the experimental period of TRAnsport and Chemical Evolution over the Pacific (TRACE-P). For model simulation, the hourly emission strength was simply by dividing above daily values over daytime hours. Two case runs with BC and OC emission sources were considered, respectively. The average BC and OC aerosol size distributions were based on the

aerosol components categorization obtained by Hess et al. (1998). In this study, we considered BC as "soot" aerosol component, and OC as "water-soluble" aerosol component, in which mode radii in dry state were approximately 0.0118 and 0.0212 μm, respectively. Dry deposition and wet scavenge were also included.

2.2 Parameterization of Biomass Burning Aerosol Optical Properties with Relative Humidity

The treatment of the parameterization of biomass burning aerosol optical properties with relative humidity was derived from the software package OPAC (Optical Properties of Aerosols and Clouds; Hess et al., 1998). In the OPAC, the aerosol optical properties such as single scattering albedo (ω), asymmetry parameter (*g*) and aerosol optical depth (τ) are calculated based on Mie theory for 61 wavelengths between 0.25 and 40 μm (Hess et al., 1998).

Table 1 lists the computed single scattering albedo (ω), asymmetry parameter (*g*) and aerosol optical depth (τ) of BC aerosol in seven wavelengths. These values were normalized to 1 particle per cubic centimeter of air within 1 km mixing layer height. For OC aerosol, we considered it as water soluble aerosol and its growth is a function of relative humidity. Figures 1 and 2 show the single scattering albedo and asymmetry parameter of OC aerosol increased with relative humidity. Above relationship for seven wavelengths at relative humidity of 0, 50, 70, 80, 90, 95, 98, and 99% can be fitted by the equation:

$$y=y_0+Ae^{RH/t}, \quad (1)$$

where *y* is the optical properties (ω or *g*), y_o is the optical properties at relative humidity 0%, *A* and *t* are numerical fit coefficients. The fit equation for each wavelength has R^2 more than 0.95. Figure 3 shows the variation of aerosol optical depth of OC aerosol with respect to relative humidity for seven wavelengths. Here we categorized relative humidity into three sections (0 - 50%, 50 - 90% and 90% - 99%). Relative humidity of 0 - 50% was fitted with liner-fit. Others were fitted with equation (1). Shows the quality of the fit obtained for 7 wavelengths with R^2 = 0.99. Overall, these aerosol optical properties values derived from parameterization are qualitatively in agreement with previous studies (Haywood et al., 2000).

Table 1. The optical properties of BC aerosol used in this study. (1 particle per cubic centimeter)

Wavelengths (λ)	ω_0	*g*	τ
UV-250 nm	3.08E-01	5.02E-01	1.35E-06
UV-300 nm	3.13E-01	4.53E-01	1.21E-06
UV-350 nm	2.91E-01	4.22E-01	1.01E-06
VIS-550 nm	2.09E-01	3.36E-01	5.51E-07
IR-1000 nm	9.65E-02	2.25E-01	2.46E-07
IR-1750 nm	3.18E-02	1.35E-01	1.30E-07
IR-5000 nm	2.40E-03	3.66E-02	4.47E-08

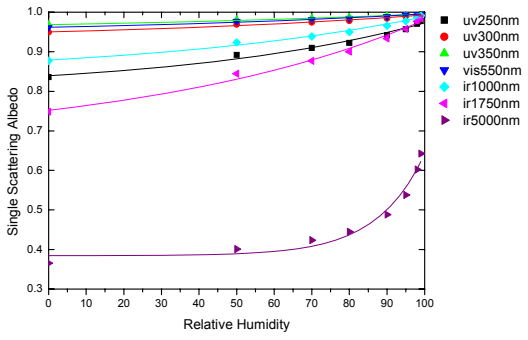

Fig 1. Variation of Single scattering albedo of OC aerosol functions of relative humidity for 7 wavelengths. (1 particle per cubic centimeter)

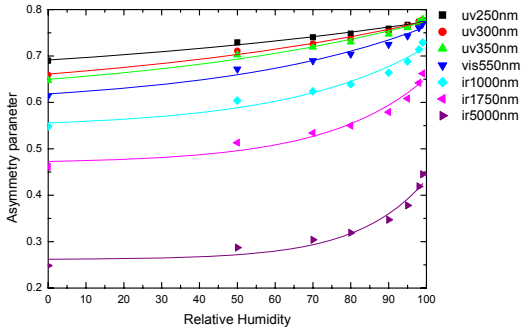

Fig 2. Variation of Asymmetry parameter of OC aerosol functions of relative humidity for 7 wavelengths. (1 particle per cubic centimeter)

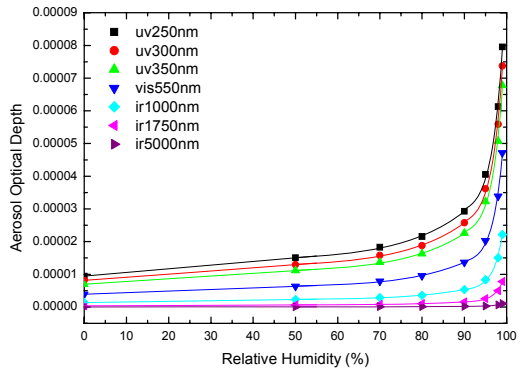

Fig 3. Variation of Aerosol Optical Depth of OC aerosol functions of relative humidity for 7 wavelengths. (1 particle per cubic centimeter)

2.3 Description of Solar Radiative Transfer Model

The mean radiative forcing of aerosol was determined by its temporal and spatial distribution in the atmosphere together with its optical properties. We used the solar radiative transfer model (CLIRAD-SW) developed by Chou and Suarez (1999) to compute the downward surface short wave flux. The model includes the absorption due to water vapor, O_3, O_2, CO_2, clouds, and aerosols. Interactions among the absorption and scattering by clouds, aerosols, molecules, and the surface are fully taken into account. Reflection and transmission of a cloud and aerosol-laden layer are computed using the δ–Eddington approximation. Fluxes are then computed using the two stream adding approximation and integrated virtually over the entire spectrum, from 0.175 to 10 μm.

3. RESULTS AND DISCUSSION

Figure 4 shows the monthly mean concentration of biomass burning aerosols (BC+OC emission) on the surface layer. Most area in Indochina and India has the concentration of biomass burning aerosols more than 1 μg m^{-3}. The maximum value reaches to 10 μg m^{-3} in northern Myanmar. Figure 5 shows mean concentration the layers between 10 m to 1000 m had similar pattern and values to that of Figure 4. It's implicated from surface to 1000 m height is well-mixed. We further analyzed the biomass burning mass concentration distributions of BC and OC aerosols were show as OC/BC ratio in Figure 6. In the southern Asia the OC/BC ratio is generally less than 7, indicating BC aerosol was relatively higher in this area.

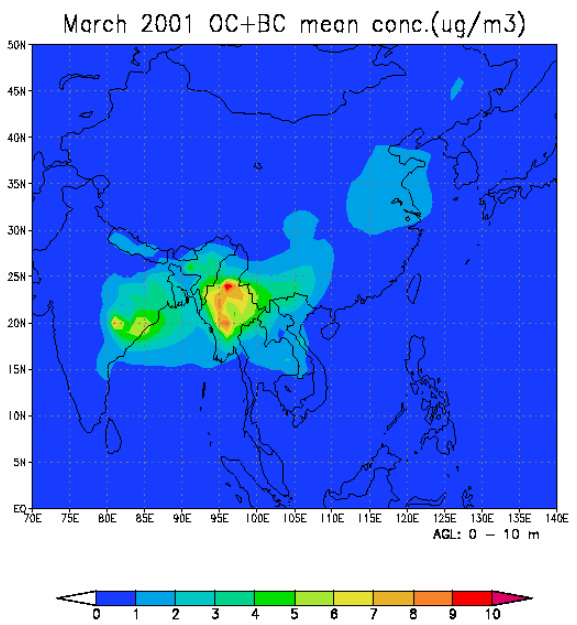

Fig 4. Simulated monthly mean mass concentration of biomass burning aerosols is on the surface layer (0 to 10 m) in March 2001. (Unit: $\mu g\ m^{-3}$)

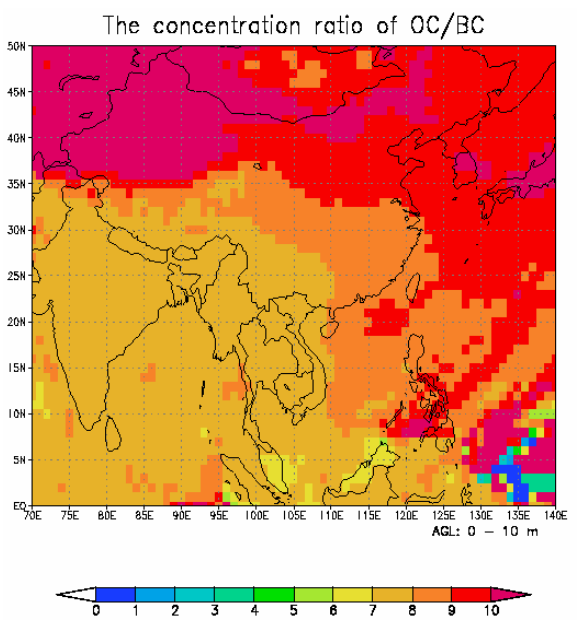

Fig 6. The mean aerosols mass concentration ratio of OC/BC at 0 to 10 m

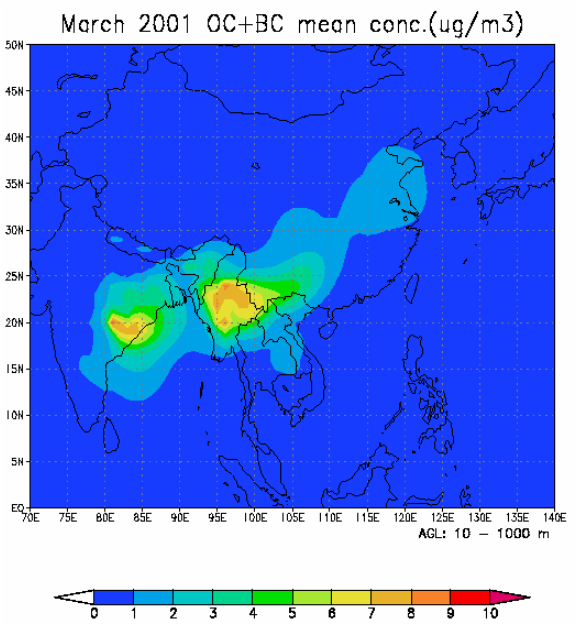

Fig 5. Simulated monthly mean mass concentration of biomass burning aerosols is at 10 to 1000 m in March 2001.

Figure 7 shows the relatively aerosol optical depth (τ) distribution of biomass burning aerosol, with maximum τ values of about 0.11 located in the western India. Figure 8 depicts the aerosol optical depth ratio of OC/BC. The ratio was less than 6 in most area especially in India (approximate to 4). The BC aerosol has relatively higher contribution to the aerosol optical depth, although the emission ratio of OC/BC (~7) is higher. It was noticed the ocean area has a higher ratio than land area, due to the increase of OC aerosol optical depth derived from higher relative humidity.

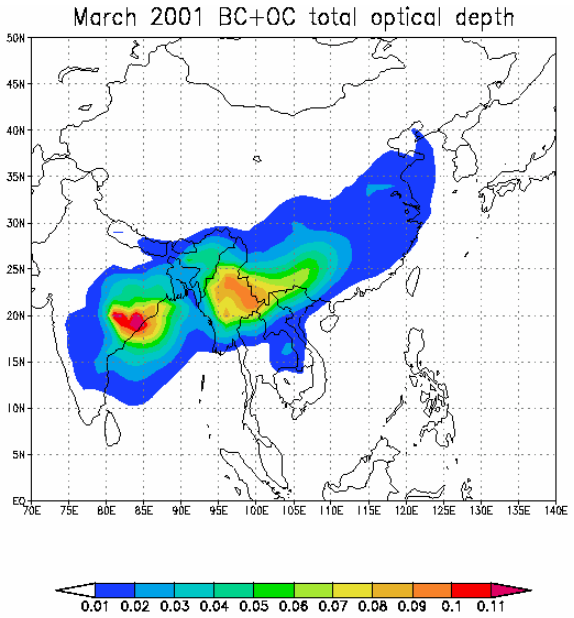

Fig 7. The aerosol optical depth (τ) of biomass burning aerosol

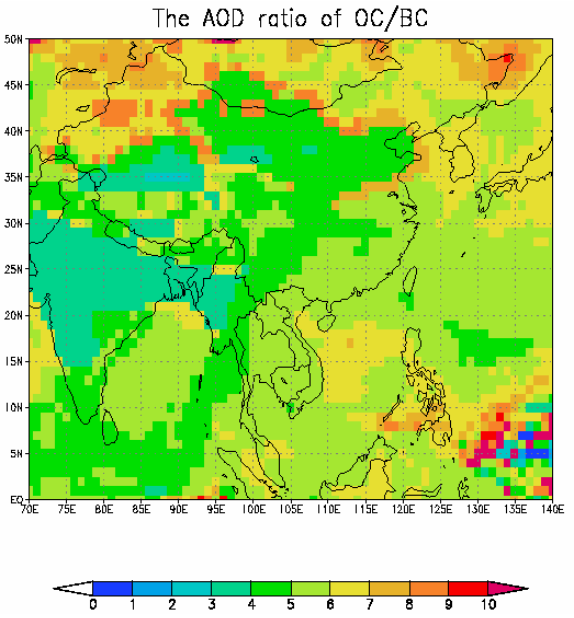

Fig 8. The aerosol optical depth ratio of OC/BC

Figures 9-10 shows the diurnal monthly mean clear sky shortwave radiative forcing due to the BC and OC aerosols from the southern Asia biomass burning. The pattern of the radiative impact is very similar to the monthly mean aerosol optical depth (Figure 7). At the TOA (Top of Atmosphere), the clear-sky TOA radiative forcing due to BC aerosol is generally positive (0 ~ 4 W m^{-2}) in source region, whereas, for OC aerosol, it can reach to as low as -7 W m^{-2}. The BC and OC aerosols warm and cool the atmosphere, respectively. At the surface layer, the clear-sky surface radiative forcing is also shown in Figure 9-10. All of the calculated results are negative. The surface radiative forcing due to BC aerosol is higher than OC aerosol. Generally, the monthly mean clear sky shortwave TOA radiative forcing ranged from 1 (land) to -5 (ocean) W m^{-2}, and surface radiative forcing ranged from -1 to -20 W m^{-2} in south and southeast Asian regions, presenting a cooling effect on the atmosphere (Figure 11).

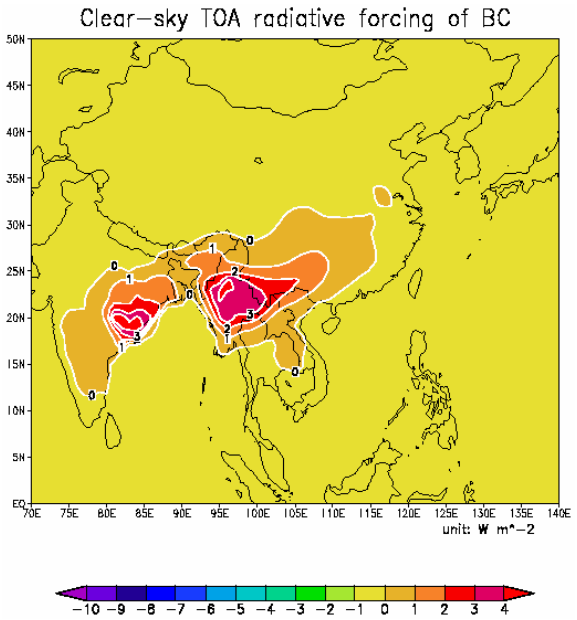

Figure 9. The monthly mean clear-sky TOA (up) and Surface (down) radiative forcing due to the BC aerosols at 550 nm.

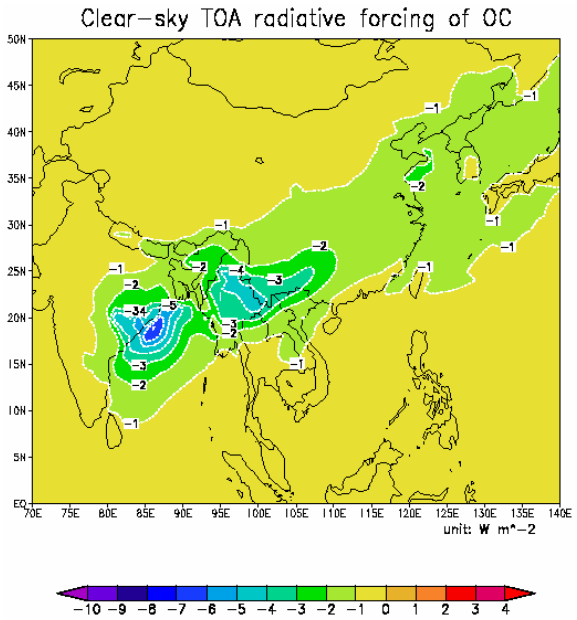

Figure 10. The monthly mean clear-sky TOA (up) and Surface (down) radiative forcing due to the OC aerosols at 550 nm.

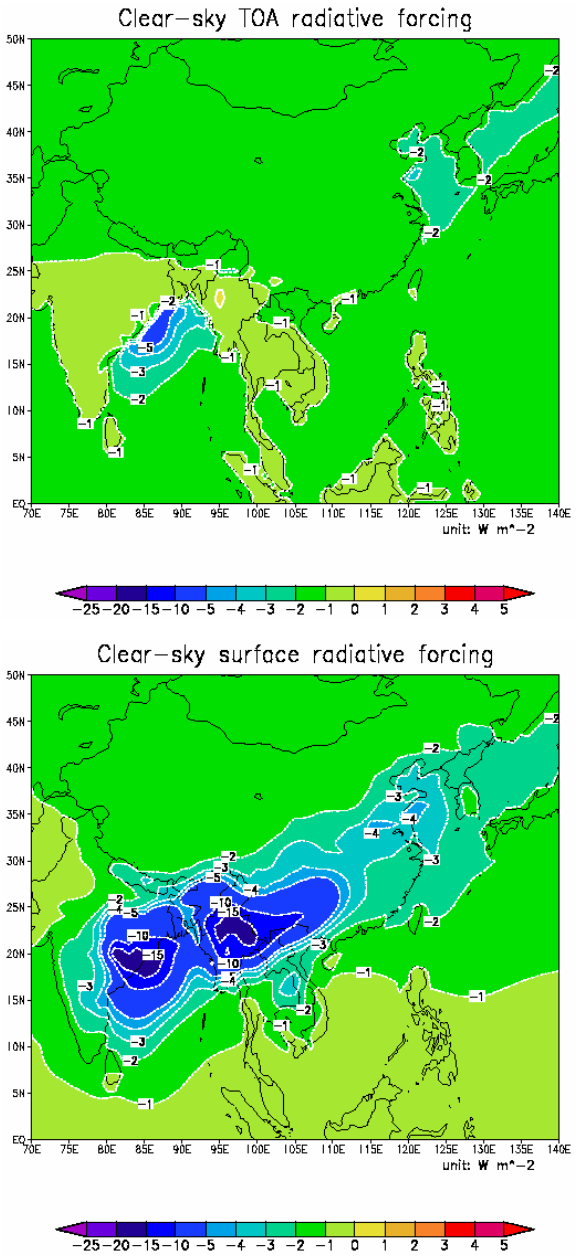

Figure 11. The monthly mean clear-sky TOA (up) and Surface (down) radiative forcing due to the biomass burning (BC+OC) aerosols at 550 nm.

In many studies, the radiative forcing was generally parameterized (Haywood et al., 2000). We further compared the radiative forcing of OC and BC aerosols calculated in this study with that of using the parameterization based on Chylek and Wong (1995):

$$\Delta F_R = S_0 \cos\theta_0 T_{atm}^2 (1-N)[(1-A)^2 2\beta\omega\tau - 4A(1-\omega)\tau] \quad (2)$$

where,

ΔF_R = the directive aerosol forcing,

S_0 = the solar constant of 1370 W m^{-2},

θ_0 = solar zenith angle,

$Tatm^2$ = the transmittance of the atmosphere, which is taken to be 0.79 (Penner et al., 1992),

N = the fraction of sky covered by clouds,

A = the surface albedo, which the global averaged A = 0.22 over the land and A = 0.06 over the ocean,

β = the upscattering fraction is calculated using an approximate relation $\beta=(1-g/2)/2$ (Sagan and Pollack, 1967),

g = asymmetry parameter,

τ = aerosol optical depth,

ω = the single scattering albedo of aerosol.

The parameters g, τ and ω were calculated in this study. Based on Eq(2), Figure 12 shows the calculated monthly mean clear-sky TOA radiative forcing due to the BC and OC aerosols at 550 nm, presenting a similar pattern to that obtained from solar radiative transfer model (see the upper panel of Figure 9 (BC) and Figure 10 (OC)). However, the later were about 60% of the former. Chylek and Wong (1995) pointed out that use of the Eq(2) should

be limited to small optical depths. And the advantage of an analytical solution in the form of Eq(2) is an explicit dependent on the individual parameters. The aerosol direct forcing can be determined by solving a more accurate from of radiation transfer model (Coakley et al., 1983).To apply Eq(2) may cause an underestimation of aerosol radiative forcing.

4. CONCLUDING REMARKS

We have successfully coupled a three-dimensional Lagrangian model (HYSPLIT) with a solar radiative transfer model (CLIRAD-SW) to estimate the radiative impact due to the aerosols from the southern Asian biomass burning. The results obtained are highlighted below:

(1) The monthly mean concentration of biomass burning aerosols presents well-mixed condition from surface to 1000 m in height and with its value ranging from 1 to 10 μg m^{-3} surrounding source regions.

(2) The derived aerosol optical depth (τ) of biomass burning aerosols has its maximum value of 0.11 in the western India. And BC aerosol had remarkable contribution to the aerosol optical depth compared with OC.

(3) At the top of atmosphere, BC aerosols cause warming effect but OC aerosols cause cooling effect. On the surface, both BC and OC cause cooling effect. Generally, the diurnal monthly mean clear sky shortwave TOA radiative forcing of biomass burning aerosols ranged from 1 (land) to -5 (ocean) W m^{-2}, and surface radiative forcing was between from -1 and -20 W m^{-2} in south and southeast Asian regions. Biomass burning aerosols in south and south-east Asian region present a cooling effect in the atmosphere.

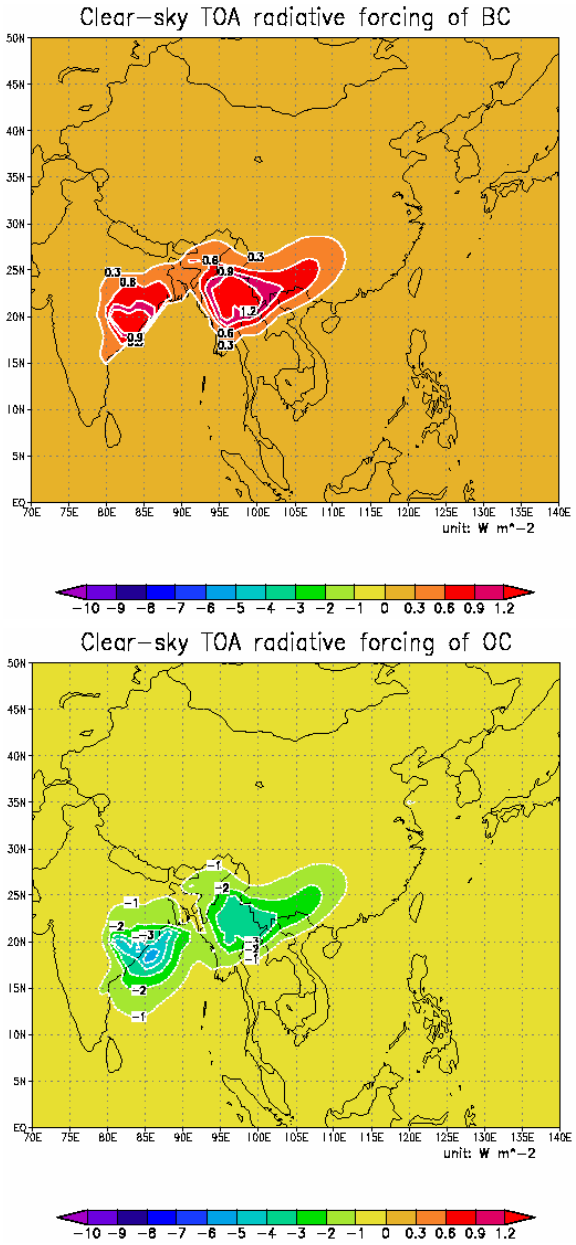

Figure 12. The monthly mean clear-sky TOA radiative forcing due to BC (up) and OC (down) aerosols at 550 nm using the Equation (2) in the text.

5. REFERENCES

Chylek, P., and J. Wong, 1995: Effect of absorbing aerosols on global radiation budget. Geophys. Res. Lett., **22**, 929-931.

Chou, M. D., and M. J., Suarez, 1999: A shortwave radiation parameterization for atmospheric studies. Technical Report Series on Global Modeling and Data Assimilation, **15**, NASA/TM-1999-104606. pp40.

Coakley, J., R. D. Cess, F. B. Yurevich, 1983: The effect of tropospheric aerosols on the earth's radiation budget: A parameterization for climate models, J. Atmos. Sci., **40**, 116-138

Draxler, R. R., Gillette, D. A., Kirkpatrick, J. S., Heller, J., 2001： Estimating PM_{10} air concentrations from dust storms in Iraq, Kuwait and Saudi Arabia. Atmos. Environ., **35**, 4315-4330.

Haywood J. M., O. Boucher, 2000: Estimates of the direct and indirect radiative forcing due to tropospheric aserosol: a review. Reviews of Geophysics, **38**, 513-543.

Hess, M., P. Koepke, and I. Schult, 1998: Optical Properties of Aerosols and Clouds: The software package OPAC. Bull. Am. Met. Soc., **79**, 831-844.

Penner, J. E., R. E. Dickinson, C. A. O'Neill, 1992: Effects of aerosol from biomass burning on the global radiation budget, Science, **256**, 1432-1434.

Intergovernmental Panel on Climate Chang (IPCC), Climate Change 2001: The Scientific Basis, edited by J. T. Houghton et al., Cambridge Univ. Press, New York.

Streets D. G., K. F. Yarber, J. H. Woo, and G. R. Carmichael, 2003: Biomass burning in Asia: annual and seasonal estimates and atmospheric emissions, Global Biogeochemical Cycles, **17**, 1099.

Sagan, C. and J, Pollack, 1967: Anisotropic nonconservative scattering and the clouds of Venus. J. Geophys. Res., **72**, 467-477.